ISSN 1674-1056
http://cpb.iphy.ac.cn
http://iopscience.iop.org/cpb
中国物理 B
Chinese Physics
中国物理
Chinese Physics B

Theoretical study on electronic structure and thermoelectric properties of PbS_xTe_{1-x} (x=0.25, 0.5, and 0.75) solid solution

Yong Lu(鲁勇), Kai-yue Li(李开跃), Xiao-lin Zhang(张晓林), Yan Huang(黄艳), Xiao-hong Shao(邵晓红)
Citation: Chin. Phys. B . 2018, 27(2): 026103. **doi:** 10.1088/1674-1056/27/2/026103

Journal homepage: http://cpb.iphy.ac.cn; http://iopscience.iop.org/cpb

What follows is a list of articles you may be interested in

Electronic structure & yield strength prediction for dislocation–Mo complex in the γ phase of nickel-based superalloys

Feng-Hua Liu(刘凤华), Chong-Yu Wang(王崇愚)
Chin. Phys. B . 2017, 26(7): 076104. **doi:** 10.1088/1674-1056/26/7/076104

Electronic and thermoelectric properties of $Mg_2Ge_xSn_{1-x}$ (x=0.25, 0.50, 0.75) solid solutions by first-principles calculations

Kai-yue Li(李开跃), Yong Lu(鲁勇), Yan Huang(黄艳), Xiao-hong Shao(邵晓红)
Chin. Phys. B . 2017, 26(6): 066103. **doi:** 10.1088/1674-1056/26/6/066103

Effects of pressure on structural, electronic, and mechanical properties of α, β, and γ uranium

Hui-Jie Zhang(张慧杰), Shi-Na Li(李世娜), Jing-Jing Zheng(郑晶晶), Wei-Dong Li(李卫东), Bao-Tian Wang(王保田)
Chin. Phys. B . 2017, 26(6): 066104. **doi:** 10.1088/1674-1056/26/6/066104

Effects of N doping on photoelectric properties of along different directions of ZnO bulk and nanotube

Zheng Hong-Mei, Fang Xiao-Yong, Cai Li-Xia, Yin Ai-Cha, Jin Hai-Bo, Yu Xiao-Xia, Cao Mao-Sheng
Chin. Phys. B . 2014, 23(12): 126102. **doi:** 10.1088/1674-1056/23/12/126102

Synthesis and thermoelectric properties of Mn-doped $AgSbTe_2$ compounds

Zhang He, Luo Jun, Zhu Hang-Tian, Liu Quan-Lin, Liang Jing-Kui, Li Jing-Bo, Liu Guang-Yao
Chin. Phys. B . 2012, 21(10): 106101. **doi:** 10.1088/1674-1056/21/10/106101

Theoretical study on electronic structure and thermoelectric properties of PbS_xTe_{1-x} ($x = 0.25$, 0.5, and 0.75) solid solution*

Yong Lu(鲁勇)†, Kai-yue Li(李开跃), Xiao-lin Zhang(张晓林), Yan Huang(黄艳), and Xiao-hong Shao(邵晓红)‡

Beijing University of Chemical Technology, College of Science, Beijing 100029, *China*

(Received 12 September 2017; revised manuscript received 28 October 2017; published online 5 January 2018)

The electronic structure and thermoelectric (TE) properties of PbS_xTe_{1-x} ($x = 0.25$, 0.5, and 0.75) solid solution have been studied by combining the first-principles calculations and semi-classical Boltzmann theory. The special quasi-random structure (SQS) method is used to model the solid solutions of PbS_xTe_{1-x}, which can produce reasonable electronic structures with respect to experimental results. The maximum zT value can reach 1.67 for p-type $PbS_{0.75}Te_{0.25}$ and 1.30 for $PbS_{0.5}Te_{0.5}$ at 800 K, respectively. The performance of p-type PbS_xTe_{1-x} is superior to the n-type ones, mainly attributed to the higher effective mass of the carriers. The zT values for PbS_xTe_{1-x} solid solutions are higher than that of pure PbTe and PbS, in which the combination of low thermal conductivity and high power factor play important roles.

Keywords: solid solution, electronic structure, thermoelectric properties

PACS: 61.50.–f, 72.15.Jf **DOI:** 10.1088/1674-1056/27/2/026103

1. Introduction

Thermoelectric (TE) materials have attracted much research interest in recent decades due to their widespread application prospects for waste heat recovery. The performance of a specific TE material is evaluated by a dimensionless figure-of-merit, $zT = \sigma S^2 T/(\kappa_l + \kappa_e)$, where S is the Seebeck coefficient, σ is electrical conductivity, T is the absolute temperature, and κ_e and κ_l are electronic and lattice thermal conductivities, respectively. For an excellent TE material with high conversion efficiency, it should combine simultaneously high values of power factor (PF), $S^2\sigma$, and low thermal conductivity. Many methods have been proposed and implemented to improve the zT values, such as formulating new structures,[1] the fabrication of superlattices or quantum dots,[2–4] doping foreign elements,[5–8] and the formation of solid solution alloying.[9,10]

PbX (X = Te and S) is one of the best materials for thermoelectric generators intended for operation at middle temperatures (from 400 K to 800 K). The high band degeneracy in the PbX materials is favorable for a high Seebeck coefficient.[11,12] Meanwhile, the strong anharmonic coupling between LA and TO phonon modes indicates that the lattice thermal conductivity can be reduced to a very low level.[13,14] Most studies have been performed to clarify or improve the performance of PbX.[15–21] For example, Dmitriev *et al.*[15] studied the PbTe using three-band model method and found a peak zT value of 0.7 and 0.6 for p-type and n-type at 700 K, respectively. Wang *et al.*[16] have then successfully synthesized n-type PbS with zT value of 0.7 at 850 K. Jin *et al.*[17] proposed a simple hydrothermal route for the synthesis of PbS–PbTe core-shell heterostructured nanorods, which produce the maximum PF of 294 $\mu W/mK^2$. Ibanez *et al.*[18] investigated the n-type $(PbTe)_{1-x}(PbS)_x$ nanocomposites and obtained the zT value of ~ 1.1 at 710 K. Korkosz *et al.*[19] studied the solid solution p-type $(PbTe)_{0.88}(PbS)_{0.12}$ and found that the phonon scattering from solid solution defects can reduce the thermal conductivity, which leads to a high zT value of 1.6 at 800 K. It is revealed that the solid solution is an effective way to improve TE performance, since it tends to cause the distortion of electronic bands[22] and introduce the nano-precipitates.[23]

In this study, we investigate the TE properties of n-type and p-type PbS_xTe_{1-x} solid solutions based on the first-principles calculations and special quasi-random structure (SQS) method.[24] The SQS method has been successfully combined with first principles to study the electronic and thermodynamic properties of disordered phases,[25–27] the basic idea of which is to produce an SQS with configurational correlation functions (CF) very close to those of solid solutions. Balancing the limitation of computer capability and calculation accuracy, we take the maximum usage of SQS-32 cell to model the disorder phase. The maximum zT value of 1.67 is obtained for p-type $PbS_{0.75}Te_{0.25}$ with a carrier concentration of 2.57×10^{19} cm^{-3} at 800 K, while the maximum zT value of n-type is 1.30 for $PbS_{0.5}Te_{0.5}$ with a carrier concentration of

*Project supported by the National Natural Science Foundation of China (Grant Nos. 11647010 and 11704020), the Higher Education and High-quality and World-class Universities (Grant No. PY201611), and the Fund for Disciplines Construction from Beijing University of Chemical Technology (Grant No. XK1702).

†Corresponding author. E-mail: luy@mail.buct.edu.cn

‡Corresponding author. E-mail: shaoxh@mail.buct.edu.cn

© 2018 Chinese Physical Society and IOP Publishing Ltd

1.34×10^{19} cm^{-3}. We believe that these valves provide reliable reference for PbS_xTe_{1-x} solid solutions since the SQS structures are very close to the real disorder state. In comparison with pure PbTe and PbS, it also provides some understanding of the effects of Te/S ratio upon electronic and TE properties.

2. Methods and computational detail

In the SQS method,[24] the pseudo-spin, $S_i = \pm1$, is introduced to assign the atom sites of the configuration occupied by A or B atom. The configurational correlation function, $f(k,m)$, is defined to group these lattice sites. The $f(k,m)$ have k vertices, where $k = 1,2,3,\ldots$ responds to point, pair, and triplet, …, respectively, and span a maximum distance of m, where $m = 1,2,3,\ldots$, is the first, second, and third nearest neighbors, etc. These correlation functions are the average product of the spin variables over all sites of a figure. The aim of the method is to find the optimum SQS with correlation functions best satisfying the condition,

$$\left(\overline{\Pi}_{k,m}\right)_{\mathrm{SQS}} \cong \langle\overline{\Pi}_{k,m}\rangle_{\mathrm{R}}, \tag{1}$$

where $\langle\overline{\Pi}_{k,m}\rangle_{\mathrm{R}}$ is the correlation function of a random alloy. For the perfectly random alloy, the pair and multisite correlation functions are given as $\langle\overline{\Pi}_{k,m}\rangle_{\mathrm{R}} = (2x-1)^k$ with x the concentration.

The PbS_xTe_{1-x} ($x = 0.25$, 0.5, and 0.75) solid solution structures are produced using the ATAT package,[28] and the corresponding electronic structures are calculated by density functional theory (DFT) as implemented in the Vienna *ab initio* Simulation Package (VASP).[29] The electron–ion interaction is described by the projector-augmented-wave (PAW) method.[30] The generalized-gradient approximation (GGA) with Perdew, Burke, and Ernzerhof (PBE) form[31] is used to describe the exchange–correlation function. The plane-wave cutoff energy is 500 eV, and the energy convergence criterion is chosen to be 10^{-5} eV. The integration over the Brillouin Zone (BZ) is done with $5\times5\times5$ Monkhorst–Pack grid meshes[32] for all the SQS-32 structures to ensure the Hellmann–Feynman forces on each ion to be less than 0.02 eV·Å^{-1}. The thermoelectric transport properties are calculated through the semi-classical Boltzmann theory and the rigid-band approach as implemented in the BoltzTrap code,[33] where the constant scattering time approximation (CSTA) is used. The CSTA method does not involve any assumption about the possible strong doping and temperature dependence of relaxation time, τ, which has been successfully applied in predicting electrical transport properties for many TE material.[34–36] In this way, the Seebeck coefficient, S, is independent of τ, while the electrical conductivity, σ, and electronic thermal conductivity, κ_e, can only be evaluated with respect to the parameter τ.

3. Results and discussion

3.1. Structural and electronic behaviors

The special quasi-random structures containing 32 atoms in the unit cell have been produced for three fractions, $x = 0.25$, 0.5, and 0.75, as shown in Fig. 1. For each fraction, the atomic positions are randomly exchanged between these lattice sites, terminated until the atomic arrangement of the unit cell converges to the closest configurational correlation functions of the random solution. These correlation functions of pairs and triplets are listed in Table 1 and the errors are estimated by $\sum(\overline{\Pi}^{\mathrm{SQS}}_{k,m} - \overline{\Pi}^{\mathrm{R}}_{k,m})^2$ up to the 7th nearest neighbors. As shown in Table 1, the correlation functions of SQS-32 unit cell for $x = 0.5$ match the random alloy statistics perfectly with no error. For $x = 0.25$ and 0.75, the error of the 7th nearest neighbors are only 0.0269, indicating that the correlation functions also match well with the random ones. The size of the SQS-32 unit cell represents a good compromise between accuracy and the computational requirements associated with the thermoelectric transport property calculations. The optimised lattice constants of these SQSs are $a = 7.87$ Å, $b = 10.22$ Å, and $c = 14.39$ Å for $PbS_{0.25}Te_{0.75}$, $a = 15.37$ Å, $b = 15.32$ Å, and $c = 4.44$ Å for $PbS_{0.5}Te_{0.5}$, and $a = 7.52$ Å, $b = 9.72$ Å, and $c = 13.74$ Å for $PbS_{0.75}Te_{0.25}$, respectively. Correspondingly, the densities are 7.73 g/cm^3 for $PbS_{0.25}Te_{0.75}$, 7.75 g/cm^3 for $PbS_{0.5}Te_{0.5}$, and 7.54 g/cm^3 for $PbS_{0.75}Te_{0.25}$, respectively. These values are close to the experimentally determined density of 7.59 g/cm^3–7.63 g/cm^3 for PbS,[37–39] but slightly lower than the density of 8.24 g/cm^3 for PbTe.[40]

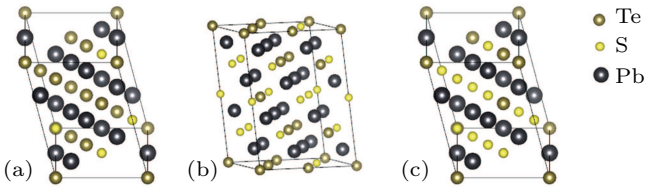


Fig. 1. (color online) The special quasi-random structures of PbS_xTe_{1-x} solid solution with (a) $x = 0.25$, (b) $x = 0.5$, and (c) $x = 0.75$, respectively. The number of atoms in the SQS unit cell is 32.

Table 1. Pair and multi-site correlation functions of SQS-32 structures. The number in the square bracket next to $\overline{\Pi}_{k,m}$ is the number of equivalent figures at the same distance in the structure. The errors were estimated by $\sum(\overline{\Pi}^{\mathrm{SQS}}_{k,m} - \overline{\Pi}^{\mathrm{R}}_{k,m})^2$ up to the 7th nearest neighbors.

	$x = 0.25$		$x = 0.5$		$x = 0.75$	
Figure	Random	SQS	Random	SQS	Random	SQS
$\overline{\Pi}_{2,1}$[06]	0.25	0.25	0	0	0.25	0.25
$\overline{\Pi}_{2,2}$[03]	0.25	0.25	0	0	0.25	0.25
$\overline{\Pi}_{2,3}$[12]	0.25	0.2292	0	0	0.25	0.2292
$\overline{\Pi}_{2,4}$[06]	0.25	0.2083	0	0	0.25	0.2083
$\overline{\Pi}_{2,5}$[12]	0.25	0.2292	0	0	0.25	0.2292
$\overline{\Pi}_{2,6}$[04]	0.25	0.375	0	0	0.25	0.375
$\overline{\Pi}_{2,7}$[24]	0.25	0.2083	0	0	0.25	0.2083
$\overline{\Pi}_{3,1}$[08]	–0.125	–0.125	0	0	0.125	0.125
$\overline{\Pi}_{3,2}$[12]	–0.125	–0.125	0	0	0.125	0.125
Error	0	0.0269	0	0	0	0.0269

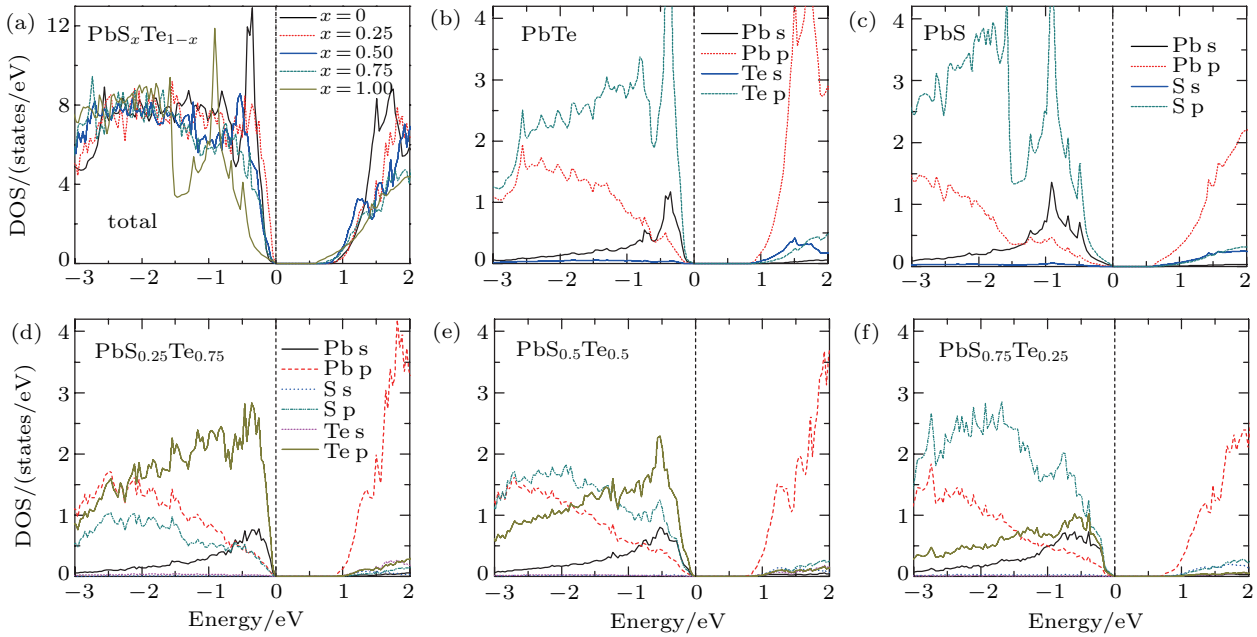


Fig. 2. (color online) The calculated electronic DOSs of PbS$_x$Te$_{1-x}$ solid solution for (a) the total DOSs, (b) pure PbTe, (c) pure PbS, (d) PbS$_{0.25}$Te$_{0.75}$, (e) PbS$_{0.5}$Te$_{0.5}$, and (f) PbS$_{0.75}$Te$_{0.25}$, respectively. All the Fermi levels are set at zero.

The total density of states (DOS) and projected DOS of PbS$_x$Te$_{1-x}$ solid solution are shown in Fig. 2, compared with those of pure PbTe and PbS. From Fig. 3(a), the slope of the total DOS at valence band maximum (VBM) is larger than that of conduction band minimum (CBM) for any compositions, indicating that the effective mass of carriers of p-type is larger than that of n-type. Since the effective mass is proportional to the Seebeck coefficient, the value of S for p-type PbS$_x$Te$_{1-x}$ is also larger than that of n-type. From the partial DOS of PbS$_x$Te$_{1-x}$ as shown in Figs. 3(b)–3(f), the conduction band is largely remarked by Pb p orbital, slightly hybridization with Te/S s and p orbitals. The valence bands show the hybridization of multiple electronic states involving Pb s, p orbitals and Te/S p orbital, indicating the occurrence of charge transfer from Pb to Te or S atoms. Through the Bader analysis,[41] we can obtain the charge transfer quantitatively, where about 2.0 electrons are transferred from Pb atom to Te atom in PbS$_{0.25}$Te$_{0.75}$ or to S atom in PbS$_{0.75}$Te$_{0.25}$. In PbTe$_{0.5}$S$_{0.5}$, the Te and S atoms are almost equivalent to sharing the electrons. Further analysis shows that these electrons are mainly from the Pb 6p orbital. As x increases from 0.25 to 0.75, the band gap (E_g) between VBM and CBM is decreased from 0.79 eV to 0.69 eV, in the range of 0.81 eV for PbTe and 0.59 eV for PbS. These data are in agreement with previous calculated values of 0.64 eV–0.83 eV for PbTe and 0.38 eV–0.50 eV for PbS.[42–44] and slightly higher than the experimental band gaps of 0.19 eV [38] and 0.30 eV for PbTe[45] and 0.41 eV for PbS[46] at room temperature.

3.2. Electrical transport properties

For metals or degenerate semiconductors with parabolic band, the S is defined as[47]

$$S = \frac{8\pi^2 k_B^2}{3eh^2} m^* T \left(\frac{\pi}{3n}\right)^{2/3}, \tag{2}$$

where k_B is the Boltzmann constant, e is the charge of one electron, h is the Planck constant, m^* is the effective mass of the carriers (holes or electrons), and n is the carrier concentration. Figures 3(a)–3(c) show the calculated Seebeck coefficient maps as a function of carrier concentration and temperature from 500 K to 800 K. It is found that the S for p-type PbS$_x$Te$_{1-x}$ is larger than that of n-type at any ratio, consistent with the larger valence-band effective mass of p-type. The absolute value of S increases with increasing temperature, while decreases with increasing carrier concentration. Due to the fact that the effective mass of the valence band is larger than the conduction band, the S of p-type PbTe$_x$S$_{1-x}$ solid solution is higher than that of n-type ones covering the whole range of concentrations considered here, as shown in Figs. 3(a)–3(c). Since the GGA method overestimates the band gap slightly with respect to experiments, we take the minimum experimental value of $E_g = 0.19$ eV for PbTe[38] to evaluate the error caused by the change of band gap. For example, at low carrier concentration of 10^{19} cm^{-3}, the Seebeck coefficient of PbS$_{0.75}$Te$_{0.25}$ decreases from 323.26 μV/K ($E_g = 0.47$ eV) to 323.03 μV/K ($E_g = 0.19$ eV) at 500 K. While at high carrier concentration of 10^{21} cm^{-3}, S decreases from 54.55 μV/K to 54.35 μV/K. The differences are both negligibly small. In the same way, it is found that the errors introduced by the change

of band gap are less than 0.5% at all temperatures and carrier concentrations considered here.

Through the electronic structure, we can directly get the σ/τ ratio as a function of carrier concentration and temperature. The electrical conductivity, σ, can then be calculated by $\sigma = (\sigma/\tau) \times \tau$. It is known that the τ is proportional to $1/T$ and $n^{-1/3}$ as a typical electron–phonon regime. The experimental data is used to simulate the behavior of τ. For p-type PbS_xTe_{1-x}, we use the data from Korkosz *et al.*,[19] in which the $(PbTe)_{0.88}(PbS)_{0.12}$ solid solution was synthesized. In this reference, the Seebeck coefficient is reported to be about 125 μV/K at 400 K. By comparing with the calculated values of S, we obtain the carrier concentration of $n = 2.42 \times 10^{20}$ cm^{-3}. Using the experimental electrical conductivity of 1.00×10^5 S/m, we obtain a relaxation time of $\tau = 3.86 \times 10^{-5} T^{-1} n^{-1/3}$. For n-type, we use the same method and choose the data from Ibánez *et al.*[18] at 710 K. Similarly, we obtain the $\tau = 2.31 \times 10^{-5} T^{-1} n^{-1/3}$. Then the electrical conductivities for PbS_xTe_{1-x} solid solutions can be obtained according to $\sigma = (\sigma/\tau) \times \tau$, which are shown in Figs. 3(d)–3(f). Clearly, the σ of the n-type is higher than that of the p-type for all these solid solutions.

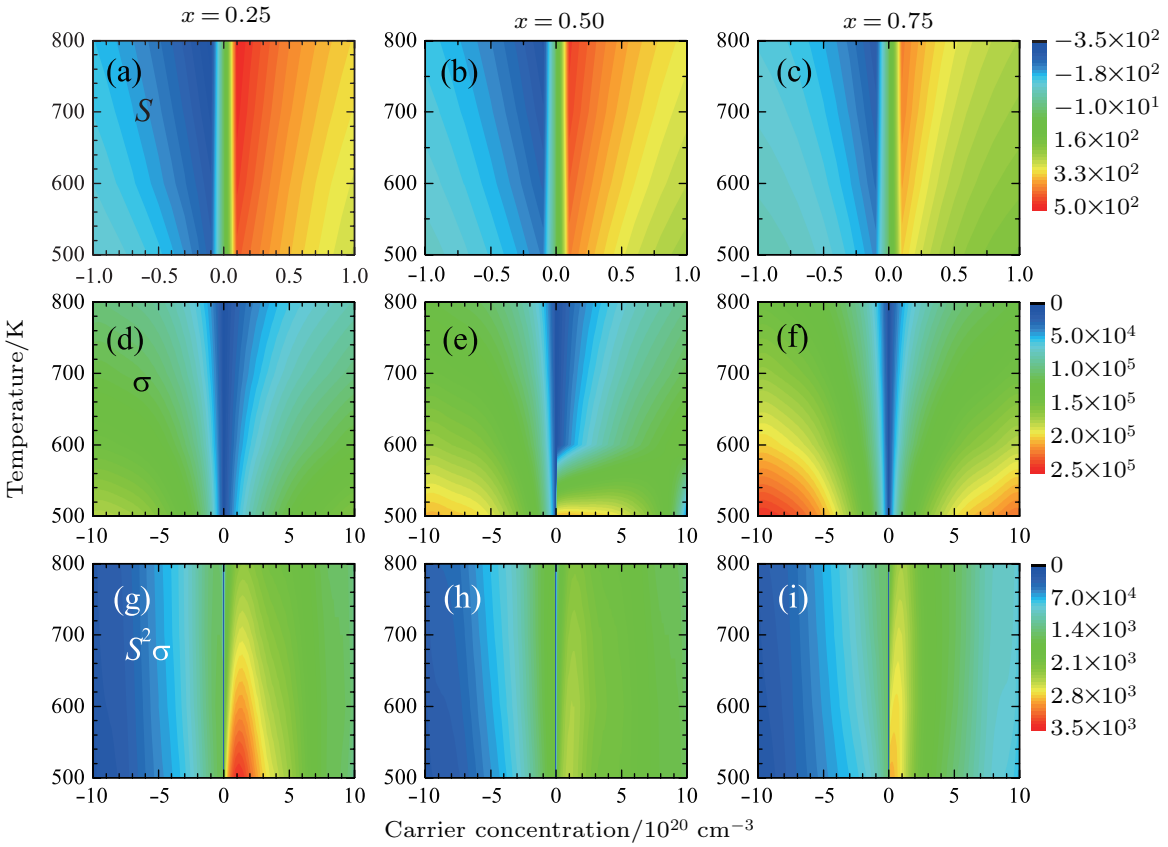


Fig. 3. (color online) Transport coefficients map of PbS_xTe_{1-x} as a function of carrier concentration and temperature for $x = 0.25$ (left), 0.50 (mid), and 0.75 (right), respectively. Panels (a)–(c) show the Seebeck coefficient, S (μV·K^{-1}); panels (d)–(f) show the electronic conductivity, σ (mΩ^{-1}·cm^{-1}); panels (g)–(f) show the power factor, $S^2\sigma$ (W·m^{-1}·K^{-2}). The negative scale of x axis stands for the n-type, while the positive scale represents the p-type.

The power factor (PF), $S^2\sigma$, can be easily obtained from the product of Seebeck coefficient and electrical conductivity, which are shown in Figs. 3(g)–3(i). As carrier concentration increases, the PF of p-type increases first and then decreases, which can be attributed to the fact that the PF is mainly affected by the σ and S at low and high carrier concentrations respectively, which show contrary trend as concentration increases. At a typical carrier concentration, these two main contributors can achieve a balance, where the PF reaches the maximum value. At 500 K, the maximum value of PF is 23 μW·cm^{-1}·K^{-2} for p-type $PbS_{0.5}Te_{0.5}$, compared to the experimental data of 21 μW·cm^{-1}·K^{-2} for p-type $PbS_{0.12}Te_{0.88}$.[19] Different from p-type, the PF of n-type shows continuous descent as concentration increases, indicating that the S plays a main role in the concentration range considered here. The PF of $PbS_{0.25}Te_{0.75}$ is 13.3 μW·cm^{-1}·K^{-2} with the carrier concentration of 4.83×10^{18} cm^{-3}, in agreement with the experimental data of 12 μW·cm^{-1}·K^{-2} for n-type $PbS_{0.12}Te_{0.88}$.[48]

The electronic thermal conductivity, κ_e, was estimated according to the Wiedemann–Franz relation, $\kappa_e = L\sigma T$, where $L = 1.8 \times 10^{-8}$ W·Ω/K^2 is the standard Lorenz number. As shown in Fig. 4, the κ_e increases rapidly as carrier concentration increases at temperature considered here. The κ_e of n-type PbS_xTe_{1-x} is higher than that of the p-type due to the higher value of σ. As temperature increases from

500 K to 800 K, the κ_e of p-type $PbS_{0.25}Te_{0.75}$ is decreased from ~ 0.9 W·m^{-1}·K^{-1} to ~ 0.6 W·m^{-1}·K^{-1}, in agreement with the experimental observations that κ_e decreases from ~ 0.7 W·m^{-1}·K^{-1} to ~ 0.3 W·m^{-1}·K^{-1} for $PbS_{0.12}Te_{0.88}$ with the carrier concentration of 10^{20} cm^{-3}.[19] For n-type $PbS_{0.25}Te_{0.75}$, the κ_e is decreased from ~ 0.5 W·m^{-1}·K^{-1} to ~ 0.4 W·m^{-1}·K^{-1}, which is consistent with the experimental data from ~ 0.75 W·m^{-1}·K^{-1} to ~ 0.45 W·m^{-1}·K^{-1} for $PbS_{0.32}Te_{0.68}$ with the carrier concentration of 6×10^{19} cm^{-3}.[18]

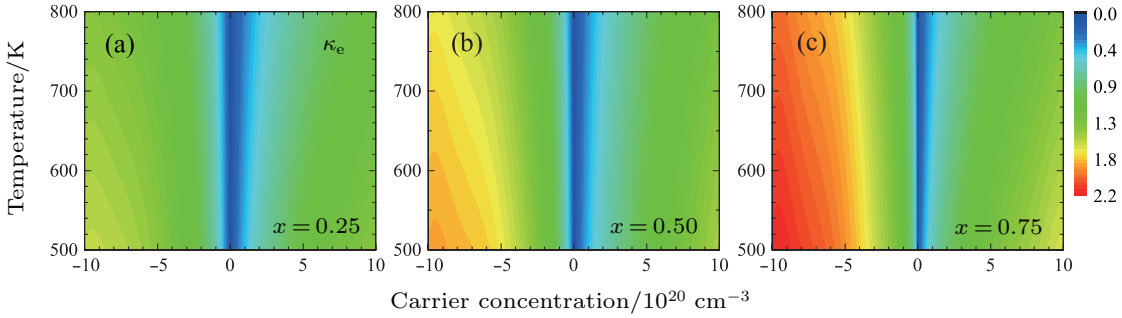


Fig. 4. (color online) Electronic thermal conductivity κ_e (W·m^{-1}·K^{-1}) map of PbS_xTe_{1-x} with (a) $x = 0.25$, (b) $x = 0.5$, and (c) $x = 0.75$ as a function of carrier concentration and temperature, respectively. The negative scale of x axis stands for the n-type, while the positive scale represents the p-type.

3.3. The zT values

The zT values of PbS_xTe_{1-x} can be calculated by the relations of $zT = \sigma S^2 T/(\kappa_l + \kappa_e)$. The experimentally determined lattice thermal conductivity of $PbS_{0.12}Te_{0.88}$[19] is used in the present calculations. According to the experimental results, as temperature increases from 500 K to 800 K, κ_l decreases from ~ 1.0 W·m^{-1}·K^{-1} to ~ 0.75 W·m^{-1}·K^{-1} following the typical $1/T$ scaling. In Fig. 5, we show the dependence of zT values upon carrier concentration from 500 K to 800 K. It is found that the zT values of p-type PbS_xTe_{1-x} are larger than those of n-type, primarily due to the higher PF of p-type PbS_xTe_{1-x}. At 800 K, zT reaches the maximum value of 1.67 for $PbS_{0.75}Te_{0.25}$ with a carrier concentration of 2.57×10^{19} cm^{-3}, slightly higher than that of $PbS_{0.25}Te_{0.75}$ (1.64) and $PbS_{0.5}Te_{0.5}$ (1.55). The calculated zT value is in agreement with the experimental data of 1.6 for $PbS_{0.12}Te_{0.88}$ at 800 K.[18] The maximum zT value of n-type is 1.30 for $PbS_{0.5}Te_{0.5}$ with a carrier concentration of 1.34×10^{19} cm^{-3}. For n-type $PbS_{0.75}Te_{0.25}$, the maximum zT value is 1.12, slightly higher than the experimental data of 1.0 for $PbS_{0.72}Te_{0.28}$.[18] The difference between theoretical and experimental results may be due to the different S/Te ratio or the lattice thermal conductivity in PbS_xTe_{1-x} solid solution. Indeed, the lattice thermal conductivity increases slightly with increasing fraction x.[19,49,50] For example, the κ_l is increased from ~ 1.0 W·m^{-1}·K^{-1} for $PbS_{0.12}Te_{0.88}$[19] to ~ 1.25 W·m^{-1}·K^{-1} for $PbS_{0.84}Te_{0.16}$[50] at 500 K. Thus, the κ_l is expanded by 25% to evaluate the error of zT. Using the enhanced values of κ_l, the obtained maximum zT values of p-type $PbS_{0.75}Te_{0.25}$ and n-type $PbS_{0.5}Te_{0.5}$ are 1.59 and 1.22 at 800 K, reduced by $\sim 4.79\%$ and $\sim 6.15\%$ respectively.

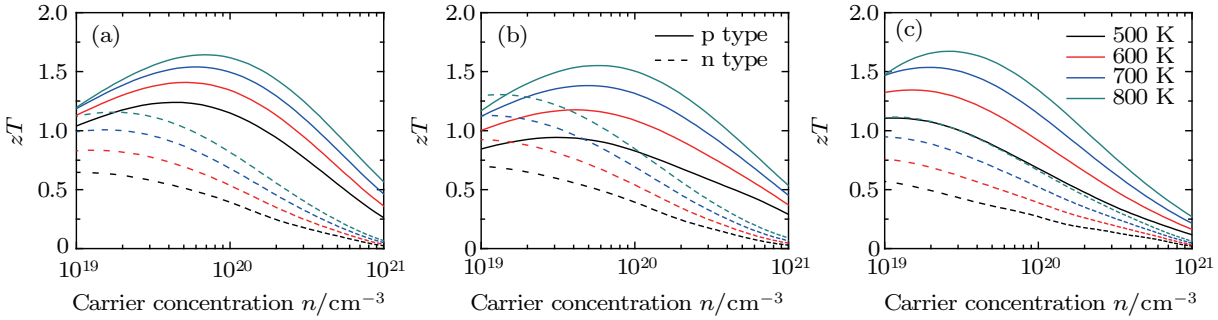


Fig. 5. (color online) Calculated zT of PbS_xTe_{1-x} with (a) $x = 0.25$, (b) $x = 0.5$, (c) $x = 0.75$ as a function of carrier concentration and temperature, respectively.

4. Conclusion

In summary, the electronic structure and thermoelectric properties of PbS_xTe_{1-x} solid solution ($x = 0.25$, 0.5, and 0.75) have been systematically studied by combining the first-principles calculations and semi-classical Boltzmann theory. The special quasi-random structure method is used to produce SQS-32 unit cell to model the PbS_xTe_{1-x} solid solution, where the configurational correlation functions match well with those of random phases. The band gap shows a tendency of decline with increasing fraction x. The effective mass of carriers for p-type PbS_xTe_{1-x} is larger than that of n-type, leading to a higher Seebeck coefficient for p-type. At a typical temperature

of 800 K, the zT reaches the maximum value of 1.67 for p-type $PbS_{0.75}Te_{0.25}$ with a carrier concentration of 2.57×10^{19} cm^{-3}, while the maximum zT value of n-type is 1.30 for $PbS_{0.5}Te_{0.5}$ with a carrier concentration of 1.34×10^{19} cm^{-3}. In general, the performance of p-type PbS_xTe_{1-x} is better than the n-type one. Compared to the pure PbTe or PbS, the thermoelectric performances of PbS_xTe_{1-x} solid solution are enhanced to a great extent.

References

[1] Kanatzidis M G 2005 *Acc. Chem. Res.* **38** 359
[2] Venkatasubramanian R, Siivola E, Colpitts T and O'Quinn B 2001 *Nature* **413** 597
[3] Venkatasubramanian R, Colpitts T, O'Quinn B, Liu S, El-Masry N and Lamvik M 1999 *Appl. Phys. Lett.* **75** 1104
[4] Harman T C, Taylor P J, Walsh M P and LaForge B E 2002 *Science* **297** 2229
[5] Kanatzidis M G, Ahn K, Li C P and Uher C 2009 *Chem. Mater.* **21** 1361
[6] Kanatzidis M G, Han M K, Hoang K, Kong H J, Pcionek R, Uher C, Paraskevopoulos K M and Mahanti S D 2008 *Chem. Mater.* **20** 3512
[7] Luo P F, Li Y, Yang J, Xing J J, Zhang J Y, Wang C Y, Zhao X L, Luo J, Zhang W Q 2017 *Chin. Phys. B* **26** 097201
[8] Zhang Y C, Liu J, Li Y, Chen Y F, Li J C, Su W B, Zhou Y C, Zhai J Z, Wang T, Wang C L 2017 *Chin. Phys. B* **26** 107201
[9] Kanatzidis M G, Poudeu P F P, D'Angelo J, Kong H J, Downey A, Short J L, Pcionek R, Hogan T P and Uher C 2006 *J. Am. Chem. Soc.* **128** 14347
[10] Kanatzidis M G, Arachchige I U, Wu J S and Dravid V P 2008 *Adv. Mater.* **20** 3638
[11] Ravich Y I 1970 *Semiconducting Lead Chalcogenides* (Plenum)
[12] Pei Y, Wang H and Snyder G J 2012 *Adv. Mater.* **24** 6125
[13] Bozin E S, Malliakas C D, Souvatzis P, Proffen T, Spaldin N A, Kanatzidis M G and Billinge S J 2010 *Science* **330** 1660
[14] Delaire O, Ma J, Marty K, May A F, McGuire M A, Du M H, Singh D J, Podlesnyak A, Ehlers G, Lumsden M D and Sales B C 2011 *Nat. Mater.* **10** 614
[15] Dmitriev A V and Tkacheva E S 2014 *Condens. Matter Phys.* **69** 243
[16] Wang J L, Wang H, Snyder G J, Zhang X, Ni Z H and Chen Y F 2013 *J. Phys. D: Appl. Phys.* **46** 405301
[17] Jin R C, Chen G, Pei J and Yan C S 2012 *New J. Chem.* **36** 2574
[18] Ibanez M, Zamani R, Gorsse S, Fan J D, Ortega S, Cadavid D, Morante J R, Arbiol J and Cabot A 2013 *ACS Nano* **7** 2573
[19] Korkosz R J, Chasapis T C, Lo S H, Doak J W, Kim Y J, Wu C I, Hatzikraniotis E, Hogan T P, Seidman D N, Wolverton C, Dravid V P and Kanatzidis M G 2014 *J. Am. Chem. Soc.* **136** 3225
[20] Lu P X, Qu L B 2013 *Chin. Phys. Lett.* **30** 017101
[21] Wang K J, Wang W, Zhang M H, Zhang X Q, Yang P, Liu B, Gao M, Huang D W, Zhang J R, Liu Y J, Wang X F, Wang F Q, He L, Xu Y B, Zhang R 2017 *Chin. Phys. Lett.* **34** 026201
[22] Heremans J P, Jovovic V, Toberer W S, Saramat A, Kurosaki K, Charoenphakdee A, Yamanaka S and Snyder G J 2008 *Science* **321** 554
[23] Androulakis J, Todorov I, He J Q, Chung D Y, Dravid V P and Kanatzidis M G 2011 *J. Am. Chem. Soc.* **133** 10920
[24] Zunger A, Wei S H, Ferreira L G and Bernard J E 1990 *Phys. Rev. Lett.* **65** 353
[25] Doak J W, Wolverton C and Ozolins V 2015 *Phys. Rev. B* **92** 174306
[26] Kim J, Kwon H, Kim J H, Roh K M, Shin D and Jang H D 2015 *J. Alloys Compd.* **619** 788
[27] Xie Y P and Zhao S J 2011 *Comput. Mater. Sci.* **50** 2586
[28] Chakraborty M, Spitaler J, Puschnig P and Ambrosch-Draxl C 2010 *Comput. Phys. Commun.* **181** 913
[29] Kresse G and Furthmoller J 1999 *Phys. Rev. B* **54** 11169
[30] Blochl P E 1994 *Phys. Rev. B* **50** 17953
[31] Perdew J P, Burke K and Ernzerhof M 1996 *Phys. Rev. Lett.* **77** 3865
[32] Monkhorst H J and Pack J D 1976 *Phys. Rev. B* **13** 5188
[33] Madsen G K H and Singh D J 2006 *Comput. Phys. Commun.* **175** 67
[34] Singh D J 2007 *Phys. Rev. B* **76** 085110
[35] Parker D and Singh D J 2011 *Phys. Rev. B* **83** 233206
[36] Parker D and Singh D J 2010 *Phys. Rev. B* **82** 035204
[37] Madelung O *et al.* 1983 *Numerical data and functional relationships in science and technology*, Landolt–Bornstei, New Series (Berlin: Springer) Vol. 17
[38] Cohen M L and Chelikowsky J R 1989 *Electronic structure and optical properties of semiconductors*, Springer Series in Solids States Sciences, 2nd edn., Vol. 75 (Berlin: Springer-Verlag)
[39] Delin A, Ravindran P, and Eriksson O 1998 *Int. J. Quantum Chem.* **69** 349
[40] Pei Y L and Liu Y 2012 *J. Alloys Compd.* **514** 40
[41] Bader R F W 1985 *Acc. Chem Res.* **18** 9
[42] Lach-Hab M *et al.* 2002 *J. Phys. Chem. Solids* **63** 833
[43] Zaoui A *et al.* 2009 *Mater. Chem. Phys.* **114** 650
[44] Boukhris N, Meradji H, Korba S A, Drablia S, Ghemid S, and Hassan F E H 2014 *Bull. Mater. Sci.* **37** 1159
[45] Girard S N, He J, Zhou X, Shoemaker D, Jaworski C M, Uher C, Dravid V P, Heremans J P, and Kanatzidis M G 2011 *J. Am. Chem. Soc.* **133** 16588
[46] Wang Y, Suna A, Mahler W, and Kasowski R 1987 *J. Chem. Phys.* **87** 7315
[47] Wang N, Li H, Ba Y, Wang Y, Wan C, Fujinami K and Koumoto K 2010 *J. Electron. Mater.* **39** 1777
[48] Li X X, Li J Q, Liu F S, Ao W Q, Li H T and Pan L C 2013 *J. Alloys Compd.* **547** 86
[49] He J Q, Girard S N, Kanatzidis M G and Dravid V P 2010 *Adv. Funct. Mater.* **20** 764
[50] Johnsen S, He J, Androulakis J, Dravid V P, Todorov I, Chung D Y, and Kanatzidis M G 2011 *J. Am. Chem. Soc.* **133** 3460